

Protective effects of acteoside against X-ray-induced damage in human skin fibroblasts

JIANHUA YANG¹, YAO YAN¹, HUIBIN LIU², JIANHUA WANG¹ and JUNPING HU³

¹Department of Pharmacy, The First Affiliated Hospital, Xinjiang Medical University; ²Department of Pharmacy, The Affiliated Tumor Hospital, Xinjiang Medical University; ³Department of Natural Medicines, School of Pharmaceutical Sciences, Xinjiang Medical University, Urumqi, Xinjiang Uyghur Autonomous Region 830011, P.R. China

Received July 2, 2014; Accepted March 16, 2015

DOI: 10.3892/mmr.2015.3630

Abstract. To investigate the protective effects of acteoside against apoptosis induced by X-ray radiation in human skin fibroblasts (HSFs), the cells were divided into the following groups: Control group; X-ray radiation group; acteoside group, in which the confluent cells were preincubated with 50 $\mu\text{g/ml}$ acteoside for 2 h followed by radiation; and positive control group, in which the cells were preincubated with 50 $\mu\text{g/ml}$ paeoniflorin followed by radiation. For the radiation, HSF cells preincubated with acteoside or paeoniflorin were exposed to X-ray beams at a dose-rate of 3 Gy/min (16 Gy in total). Cell viability, apoptosis and intracellular alteration of redox were monitored by MTT and flow cytometry. Compared with the radiation group, the number of cells arrested at the G0/G1 phase was significantly reduced in the acteoside and paeoniflorin groups, respectively ($P < 0.05$). X-ray radiation induced marked apoptosis in HSF cells and acteoside reversed this effect. Compared with the radiation group, the generation of intracellular reactive oxygen species (ROS) was abrogated by pre-incubation with acteoside or paeoniflorin ($P < 0.05$). In addition, the upregulation of pro-caspase-3 induced by radiation was reversed by acteoside or paeoniflorin. Radiation could induce upregulation of Bax and downregulation of Bcl-2; however, it was reversed completely after administration of acteoside or paeoniflorin. Furthermore, the enhanced expression of ERK and JNK induced by radiation was reversed by acteoside or paeoniflorin. Acteoside could protect the cells from X-ray induced damage through enhancing the scavenging activity of ROS, decreasing the Bax/Bcl-2 ratio and downregulating the activity of procaspase-3, as well as modulating the mitogen-activated protein kinase signaling pathways.

Introduction

Radiotherapy is a common therapeutic strategy for cancer. However, its effectiveness is usually limited by the inherent sensitivity of normal tissue to ionizing radiation, which contributes to the generation of a large number of oxidizing free radicals causing irreversible cell apoptosis (1). Therefore, it is necessary to develop novel strategies to prevent radiation-induced apoptosis of normal cells.

Cistanche, a genus of parasitic plants mainly distributed in arid lands and desert, have been commonly used as a traditional Chinese herbal medicine for treating various disorders, including renal deficiency, morbid leucorrhea, chronic infection and hematopoietic disorders (2). Extensive studies have been conducted to investigate the biological and physiochemical properties of *Cistanche*, which revealed that it exhibited neuroprotective, anti-inflammatory, antioxidant and antiaging effects (3). The stems of *Cistanche salsa*, a parasitic plant native to the northwest China with phenylethanoid glycosides (PhGs) as the major active components, have been considered as an important traditional Chinese herbal medicine for treating renal dysfunction and neurasthenia (4). Acteoside, one type of PhG derived from *Cistanche* showed antioxidative, hepatoprotective, antiviral, antimetastasis, and anti-inflammatory properties (5-7). However, few studies have been performed to investigate its protective effects against radiation-induced damage.

The present study aimed to investigate the inhibitory effects of acteoside on radiation-induced apoptosis in human skin fibroblasts and the underlying mechanism

Materials and methods

Materials. Human skin fibroblasts (HSFs) were purchased from Fuxiang Biotechnology Co., Ltd. (Shanghai, China). Dulbecco's modified Eagle's medium (DMEM) was obtained from Sangon Biotech Co., Ltd. (Shanghai, China). Fetal bovine serum (FBS) was provided by Sangon Biotech (Shanghai, China). Antibodies against procaspase-3 (cat. no. sc-7148), Bcl-2 (cat. no. sc-783), Bax (cat. no. sc-493), JNK (cat. no. sc-7345), p-JNK (cat. no. sc-6254), ERK (cat. no. sc-94), p-ERK (cat. no. sc-7383) and β -actin (cat. no. sc-47778) were purchased from Santa Cruz Biotechnology Inc. (Santa Cruz, CA, USA).

Correspondence to: Professor Junping Hu, Department of Natural Medicines, School of Pharmaceutical Sciences, Xinjiang Medical University, 393 Xinyi Road, Urumqi, Xinjiang Uyghur Autonomous Region 830011, P.R. China
E-mail: hjp-yft@163.com

Key words: acteoside, paeoniflorin, radiation, mitogen-activated protein kinase signal pathway, apoptosis

Extraction and identification of acteoside. *Cistanche salsa* (C.A. Mey.) G. Beck (10 kg) was extracted with ethanol as previously described (8). Then the mixture was concentrated, and the residue was suspended in water, followed by extraction with ethyl acetate and n-butyl alcohol. The n-butyl alcohol fraction was isolated by an SP825 chromatograph system (Sigma-Aldrich, St. Louis, MO, USA). Acteoside (825 mg) was isolated by further separation over Sephadex LH-20 (Sigma-Aldrich, St. Louis, MO, USA). The structure of acteoside (Fig. 1) was identified by spectroscopic techniques (HPLC and NMR) (9). The purity of acteoside was $\geq 99\%$ based on the HPLC analysis with a wavelength of 333 nm.

Cell culture. HSF cell line was cultured in Dulbecco's modified Eagle's medium supplemented with 10% fetal bovine serum, 100 U/ml penicillin and 100 $\mu\text{g/ml}$ streptomycin (Sigma-Aldrich) at 37°C in a humidified atmosphere of 5% CO₂-95% air. The cells were harvested and prepared for further analysis once exponential growth was achieved.

Experimental design. The cells were divided into: i) Control group, which was subjected to no radiation; ii) radiation group, in which the cells were only subjected to radiation; iii) experimental group, in which the confluent cells were preincubated with 50 $\mu\text{g/ml}$ acteoside for 2 h followed by radiation; and (iii) positive control group, in which the cells were preincubated with 50 $\mu\text{g/ml}$ paeoniflorin followed by radiation. For the radiation, HSF cells preincubated with acteoside or paeoniflorin were exposed to X-ray beams with a dose-rate of 3 Gy/min generated from a Varian 2300 C/D medical linear accelerator (Varian Medical Systems Inc., Palo Alto, CA, USA). The radiation field was 25x25 cm at the isocenter in the plane perpendicular to the beam. The total dose for the radiation was 16.0 Gy.

MTT assay. Cell survival after radiation was determined using an MTT assay as previously described (10). In brief, 2×10^4 cells were plated in 200 μl culture medium in 96-well plates and incubated for 48 h. At the indicated time points (2, 24, 48 and 72 h after radiation), a total of 20 μl MTT (Sigma-Aldrich) solution in phosphate-buffered saline was added to each well. After 4 h of incubation, the supernatant was removed and 150 μl dimethyl-sulfoxide was added to each well to terminate the reaction. The absorbance at 570 nm was determined using a Biokinetics plate reader (BioTek Instruments, Inc., Winooski, VT, USA).

Annexin V assay for apoptosis. Cellular apoptosis was determined using an Annexin V-fluorescein isothiocyanate (FITC) apoptosis detection kit (Invitrogen Life Technologies, Grand Island, NY, USA). In brief, 1×10^6 cells were harvested and washed with PBS. Then the cells were resuspended in 500 μl binding buffer. Subsequently, the cells were incubated in 5 μl Annexin V-FITC and 10 μl propidium iodide (PI) solution for 5 min at room temperature in the dark. Finally, FITC fluorescence was analyzed by Expose ADC software (Beckman-Coulter, San Diego, CA, US).

Cell cycle analysis. Cell cycle analysis was performed using a FACScan flow cytometer (Becton Dickinson

Immunocytometry Systems, San Jose, CA, USA). The cells were then washed with PBS (pH 7.4) and fixed with 70% ice-cold ethanol at 4°C overnight. After that, the cells were stained with PI solution (20 $\mu\text{g/ml}$) for 15 min at room temperature. The percentage of cells in G1, S and G2/M phase of the cell cycle was determined according to a previous study (11). Data acquisition and analysis were controlled by CellQuest version 5.2 software (BD Biosciences, San Diego, CA, USA).

Determination of ROS level. Generation of intracellular ROS was assessed as described by Cathcart *et al.* (12). Briefly, after radiation, HSF obtained from the groups were incubated with 10 μM DCFH-DA (Sigma-Aldrich) for 30 min. Subsequently, ROS production was measured using a flow cytometer (Beckman-Coulter, San Diego, CA, USA). The intensity of dichlorofluorescein (DCF) fluorescence was measured with an excitation wavelength and an emission wavelength of 485 and 530 nm, respectively.

Western blot analysis. Western blot analysis was performed as previously described (13). In brief, the cells were treated with 0.5 ml radioimmunoprecipitation assay (RIPA) lysis buffer (Beijing ComWin Biotech Co., Ltd., Beijing, China), followed by centrifugation at 16,363 x g at 4°C for 15 min. The obtained proteins (100 μg) were separated by electrophoresis on a 10% SDS-PAGE gel and transferred to a Hybond-P polyvinylidene difluoride (PVDF) membrane (EMD Millipore, Bedford, MA, USA). Then the membrane was blocked with 5% (w/v) non-fat dry milk and incubated with primary antibodies against procaspase-3 (1:200), Bcl-2 (1:200), Bax (1:200), JNK (1:200), p-JNK (1:200), ERK (1:200), p-ERK (1:200), and β -actin (1:3,000, Fude Biological Technology, Hangzhou, China) overnight at 4°C. Then the mixture was incubated with horseradish peroxidase-conjugated goat anti-mouse IgG (1:5,000; Fude Biological Technology; cat. no. FD-GAM007) for 1 h at room temperature. After washing with PBS, the bound primary antibody was visualized with the Enhanced Chemiluminescence system from Amersham (Piscataway, NJ, USA) and exposed to film. The same membrane was probed for β -actin (Boster Corporation, Wuhan, China), a loading control. The relative density of proteins to β -actin was analyzed with the AlphaEaseFC software (Genetic Technologies, Inc. Miami, FL, USA).

Statistical analysis. All data are presented as the mean \pm standard deviation (SD). SPSS 16.0 software (SPSS Inc., Chicago, IL, USA) was used for data analysis. Analysis of variance was conducted to compare the inter-group difference. $P < 0.05$ was considered to indicate a statistically significant difference.

Results

Effect of acteoside on the viability of HSF. A marked decrease was noted in the cellular viability of cells exposed to X-ray beams compared with the normal control at 48 ($P < 0.05$) and 72 h ($P < 0.05$), respectively (Table I). For the cells pretreated using various concentrations of acteoside, higher cell survival rates were obtained than that of radiation group (Fig. 2).

Table I. Proliferation activity indicated by OD₅₇₀ value of human skin fibroblasts.

Incubation time (h)	OD ₅₇₀		
	Control group	Radiated group	Acteoside group
2	0.288±0.025	0.280±0.023	0.421±0.058 ^b
24	0.306±0.020	0.287±0.025	0.547±0.072 ^b
48	0.437±0.037	0.358±0.020 ^a	0.445±0.079 ^c
72	0.576±0.075	0.425±0.076 ^a	0.585±0.073

^aP<0.01 vs. control group; ^bP<0.01 and ^cP<0.05 vs. radiated group.

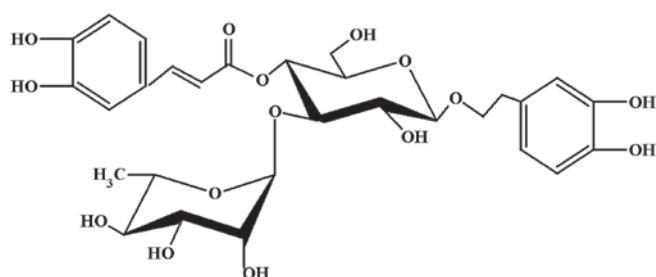


Figure 1. Chemical structure of acteoside.

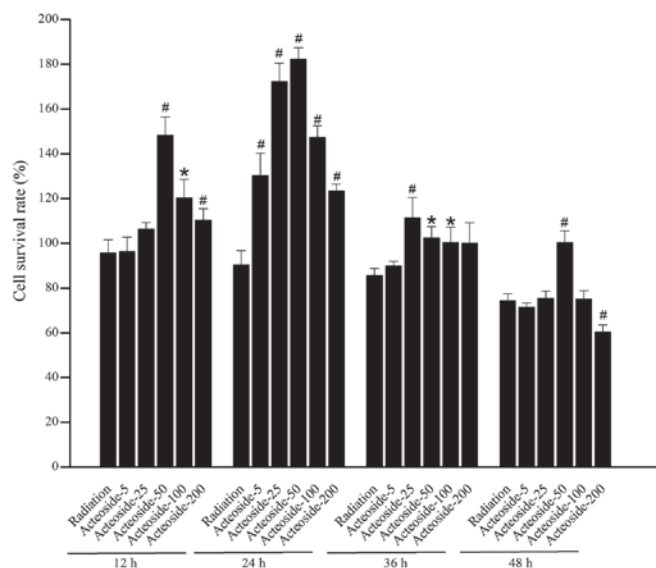


Figure 2. Effect of acteoside on X-ray-induced cytotoxicity in human skin fibroblasts. Cell viability was measured using the MTT assay and expressed as the percentage of treated samples to control samples. Data are represented as the mean ± standard deviation. *P<0.05 and #P<0.01, vs. the radiation group.

Effect of acteoside on cell apoptosis. To investigate whether the reduction in cell viability was due to apoptosis, cytometric analysis was performed using a flow cytometer. As shown in Fig. 3, a significant increase was observed in the apoptosis of cells subjected to radiation compared with the control group (P<0.05). Conversely, the apoptosis rates in the acteoside and paeoniflorin groups were significantly reduced compared with that of the radiation group (P<0.05).

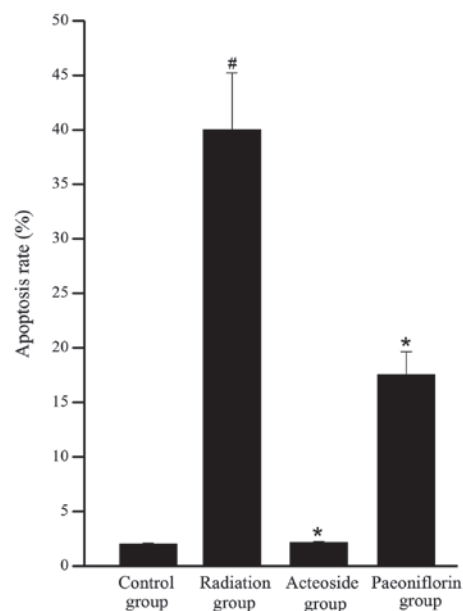


Figure 3. Effect of acteoside on X-ray-induced apoptosis in human skin fibroblasts. Flow cytometry was performed to determine the vitality of cells in the control group, radiation group (subjected to 16.0 Gy radiation for 2 h), acteoside group (preincubated with 50 µg/ml acteoside for 2 h followed by radiation) and paeoniflorin group (preincubated with 50 µg/ml paeoniflorin for 2 h followed by radiation), respectively. Apoptosis was induced by X-ray radiation, while the interference of acteoside or paeoniflorin could reverse the apoptosis induced by radiation. Data are presented as the mean ± standard deviation. #P<0.01, vs. control; *P<0.01, vs. radiation group.

Effect of acteoside on the cell cycle. Fig. 4 shows the distribution of cells in different phases of the cell cycles in each group. Compared with the control group, the majority of the cells subjected to X-ray radiation were arrested at the G₀/G₁ phase, and few cells were arrested at S phase or G₂/M phase. For the irradiated cells pre-incubated with acteoside, the number of cells blocked at G₀/G₁ phase was reduced compared with that of the radiation group (P<0.05).

Effect of acteoside on cell production of ROS. As shown in Fig. 5, the level of DCFH-DA in the cells treated with X-ray was 1.8-fold higher than that of the control group (P<0.01). Compared with the radiation group, the generation of ROS was completely abrogated by pre-incubation with acteoside or paeoniflorin (P<0.05).

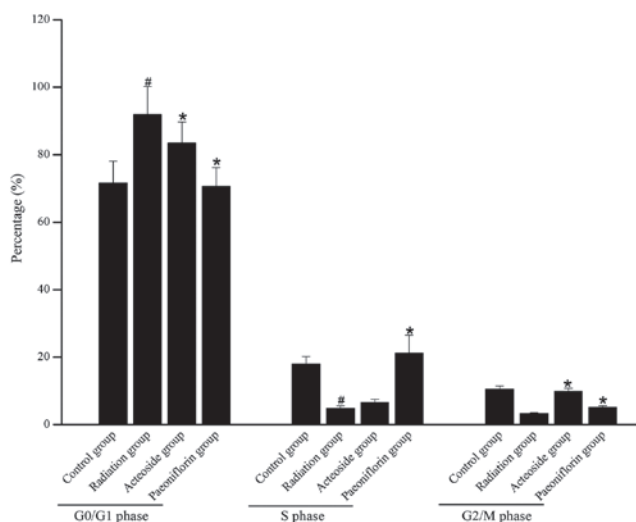


Figure 4. Effect of acteoside on X-ray-induced cell cycle perturbation in human skin fibroblasts. The cell cycle distribution was calculated in the control group, radiation group, acteoside group and paeoniflorin group by CellQuest software. Data are presented as the mean \pm standard deviation of three independent experiments. [#] $P < 0.05$, vs. control; ^{*} $P < 0.05$, vs. the radiation group.

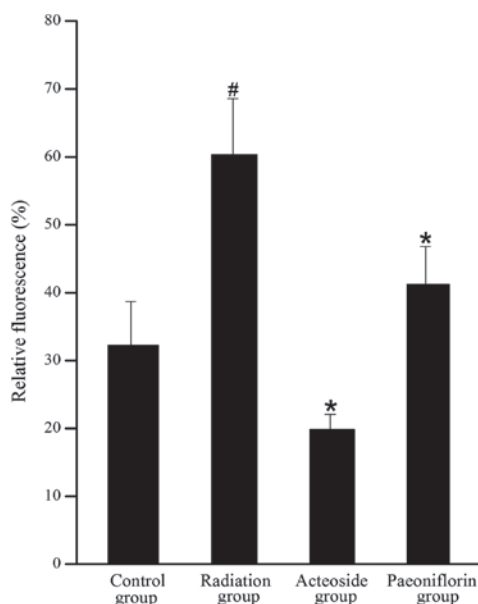


Figure 5. Protective effects of acteoside on radiation mediated ROS production in human skin fibroblasts. The cells were divided into the control group, radiation group, acteoside group and paeoniflorin group, respectively. Intracellular ROS was calculated by CellQuest software according to the relative fluorescence. Data are presented as the mean \pm standard deviation of three independent experiments. [#] $P < 0.01$ vs. control; ^{*} $P < 0.01$ vs. the irradiation group. ROS, reactive oxygen species.

Expression of apoptosis-associated proteins. To investigate the effects of acteoside on the expression of apoptosis-associated proteins, the expression of procaspase-3, Bax, Bcl-2, p-ERK, ERK, p-JNK and JNK, was determined. For the cells subjected to radiation, expression of procaspase-3 was downregulated compared with that of the control group ($P < 0.01$, Fig. 6). However, compared with the radiation group, expression of procaspase-3 showed marked increase in the cells preincubated with acteoside or paeoniflorin ($P < 0.01$). Compared with the

radiation group, cells treated using acteoside or paeoniflorin showed significant increase in the radiation group ($P < 0.05$). The expression of Bax was significantly upregulated in cells subjected to radiation compared with that of the control group ($P < 0.01$). Nevertheless, for the cells preincubated with acteoside or paeoniflorin, a significant decrease was noted in the expression of Bax compared with the radiation group ($P < 0.05$). In addition, the radiation group showed a significant decrease in the expression of Bcl-2 compared with the control group ($P < 0.01$), and this phenomenon was reversed in the acteoside and paeoniflorin groups. The phosphorylation levels of ERK and JNK were significantly increased after radiation compared with that of the control group ($P < 0.01$). However, the enhanced expression of phosphorylated ERK and JNK was totally reversed by prior treatment with acteoside or paeoniflorin at 50 $\mu\text{g/ml}$.

Discussion

C. salsa has been widely used in the treatment of renal dysfunction and malnutrition (14). This study focused on the protective effects of acteoside, an active component extracted from *C. salsa*, on the radiation-induced apoptosis *in vitro*. The results demonstrated that acteoside could attenuate the apoptosis induced by X-ray beams through the removal of ROS, and involved in the modulation of the mitogen-activated protein kinase (MAPK) signaling pathway.

In previous studies, paeoniflorin has been reported to show various pharmacological activities, including inhibiting apoptosis (15,16). In this study, paeoniflorin was set as a positive control, based on which to investigate the effects of acteoside on radiation-induced injury. On this basis, the cell survival rates of irradiated cells preincubated with paeoniflorin and acteoside (with a concentration of 5, 25, 50, 100 and 200 $\mu\text{g/ml}$, respectively) were compared. The results showed that acteoside could attenuate the cellular apoptosis of cells that underwent radiation treatment. To investigate the potential mechanism underlying this effect, the abrogation of intracellular reactive oxygen species, the regulation of Bcl-2 family members, the activation of caspases, as well as the modulation of MAPK signaling pathways were determined.

Overproduction of ROS has been considered as the major cause of oxidative stress, which results in apoptosis, aging, tissue inflammation and degeneration (17). The scavenging activity of ROS has been considered to contribute to the apoptosis-inhibiting effects *in vivo* and *in vitro* (18). In the present study, HSF preincubated with acteoside showed a significant decrease in the generation of intracellular ROS. Therefore, it was hypothesized that acteoside-induced cell protection may be correlated with the scavenging effects on oxygen radicals. In addition, the assumption is strongly supported by the results that acteoside could effectively block the radiation-induced expression of apoptosis-related proteins.

The susceptibility of cells to death signals is dependent, in part, on the ratio between pro-apoptotic and anti-apoptotic Bax/Bcl-2 proteins (19). Bcl-2 acts to prevent the release of cytochrome *c* and caspase activation, while Bax has the opposite function, which in turn promotes the release of cytochrome *c* into the cytosol from mitochondria and activates caspase 3 (20,21). For the cells preincubated with acteoside

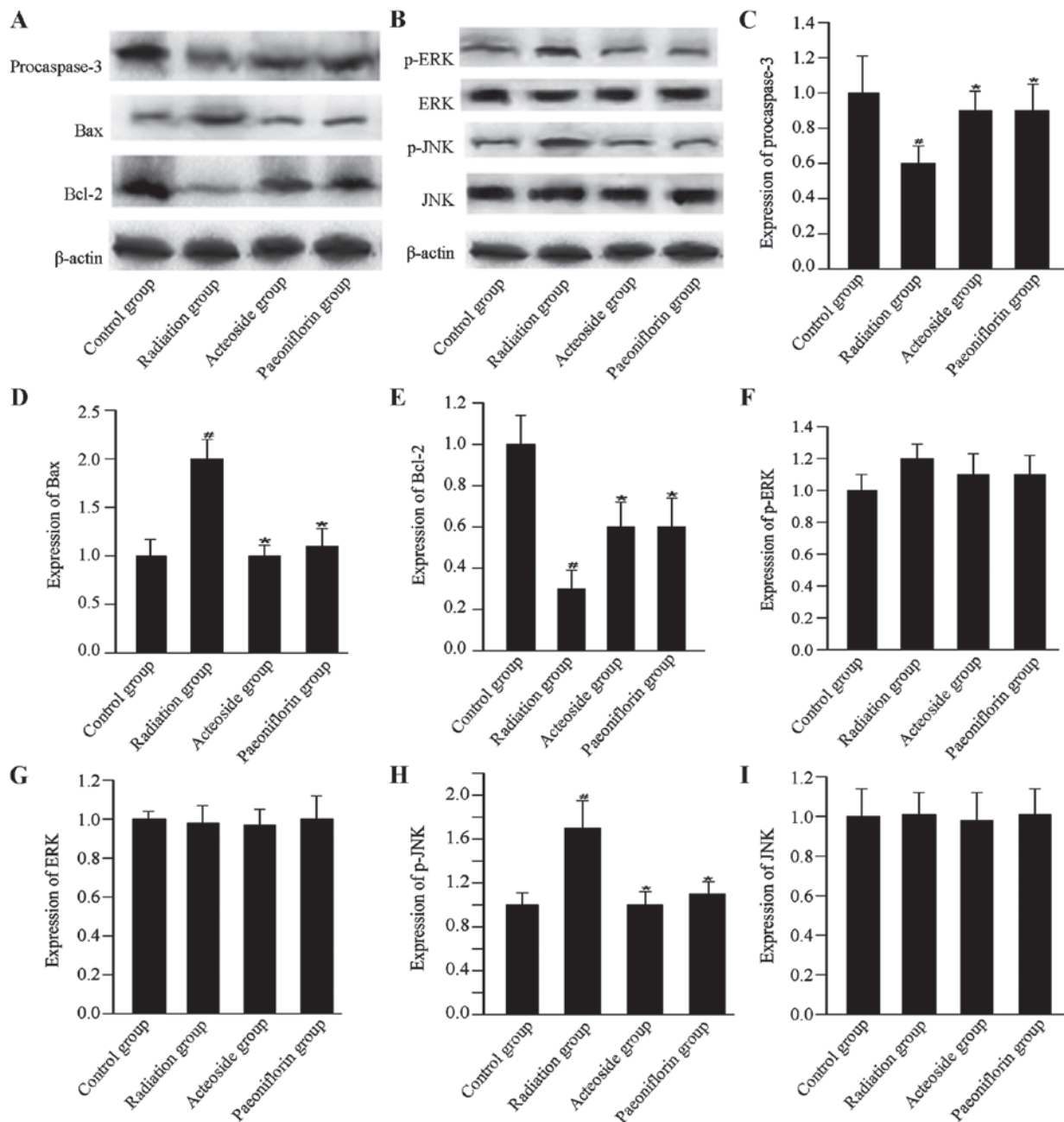


Figure 6. Effect of acteoside on the expression of apoptosis-related proteins using western blot analysis. (A) Levels of apoptosis-targeted proteins, including procaspase-3, Bax and Bcl-2 in the control group, radiation group, acteoside group and paeoniflorin group. (B) Levels of apoptosis-targeted proteins, including p-ERK, ERK, p-JNK and JNK were examined using western blot. The quantification of (C) procaspase-3, (D) Bax, (E) Bcl-2, (F) p-ERK, (G) ERK, (H) p-JNK, and (I) JNK was normalized to β -actin. * $P < 0.01$ vs. control; * $P < 0.01$ vs. the irradiation group.

prior to radiation, the ratio of Bax/Bcl-2 decreased compared with the cells that underwent radiation. This indicated that acteoside was pivotal in apoptosis through inhibiting the X-ray mediated Bax/Bcl-2 imbalance. Additionally, the decreased expression of procaspase-3 induced by X-ray radiation was reversed by pretreatment with acteoside. These results indicated that acteoside could, at least in part, inhibit X-ray-induced apoptosis in HSF cells.

The MAPK signaling pathway is important in the transmission of extracellular signals to the nucleus. To the best of our knowledge, there are three classes of MAPKs in mammals, JNK, ERK and p38 MAPK. Generally, the activation of ERK contributed to cell proliferation, while activation

of JNK and/or p38MAPK is important in the regulation of cell death (22). To date, the mechanism of how acteoside is involved in the inhibition of cellular apoptosis is still not well defined. In a previous study, Pu *et al* (23) reported that acteoside extracted from *C. salsa* could inhibit the cellular apoptosis induced by 1-methyl-4-phenylpyridinium ion in cerebellar granule neurons by inhibiting caspase activation. However, the role of acteoside in the regulation of the MAPK signaling pathway is still not well defined. In our study, the expression of p-JNK was upregulated in the acteoside group compared with the radiation group. Additionally, the increased expression of p-ERK may contribute to the cellular proliferation. All these facts may contribute to the protective effects

of acteoside on the inhibition of radiation induced apoptosis. The results strongly suggested that acteoside treatment could attenuate or counteract the radiation damage in HSF cells.

In conclusion, this study demonstrates that acteoside could protect the human skin fibroblasts from X-ray induced apoptosis by scavenging the intracellular ROS, decreasing Bax/Bcl-2 ratio and downregulating the activity of procaspase-3, as well as modulating the MAPK signaling pathways.

Acknowledgements

This study is supported by the National Nature Science Foundation of China (grant no. 81060333), the National Nature Science Foundation of China (grant no. 81360670) and the Application and Development Program Foundation from Technology Board of Urumqi (grant no. Y111310032).

References

1. Mothersill C and Seymour C: Radiation-induced bystander effects: are they good, bad or both? *Med Confl Surviv* 21: 101-110, 2005.
2. Jiang Y and Tu PF: Analysis of chemical constituents in *Cistanche* species. *J Chromatogr A* 1216: 1970-1979, 2009.
3. Xuan GD and Liu CQ: Research on the effect of phenylethanoid glycosides (PEG) of the *Cistanche deserticola* on anti-aging in aged mice induced by D-galactose. *Zhong Yao Cai* 31: 1385-1388, 2008 (In Chinese).
4. Geng X, Song L, Pu X and Tu P: Neuroprotective effects of phenylethanoid glycosides from *Cistanches salsa* against 1-methyl-4-phenyl-1,2,3,6-tetrahydropyridine (MPTP)-induced dopaminergic toxicity in C57 mice. *Biol Pharm Bull* 27: 797-801, 2004.
5. Koo KA, Kim SH, Oh TH and Kim YC: Acteoside and its aglycones protect primary cultures of rat cortical cells from glutamate-induced excitotoxicity. *Life Sci* 79: 709-716, 2006.
6. He ZD, Lau KM, Xu HX, Li PC, Pui-Hay and But P: Antioxidant activity of phenylethanoid glycosides from *Brandisia hancei*. *J Ethnopharmacol* 71: 483-486, 2000.
7. Diaz AM, Abad MJ, Fernández L, Silván AM, De Santos J and Bermejo P: Phenylpropanoid glycosides from *Scrophularia scorodonia*: in vitro anti-inflammatory activity. *Life Sci* 74: 2515-2526, 2004.
8. Lei L, Yang F, Zhang T, Tu P, Wu L and Ito Y: Preparative isolation and purification of acteoside and 2'-acetyl acteoside from *Cistanches salsa* (C.A. Mey.) G. Beck by high-speed counter-current chromatography. *J Chromatogr A* 912: 181-185, 2001.
9. Li Y, Gan L, Li GQ, Deng L, Zhang X and Deng Y: Pharmacokinetics of plantamajoside and acetoside from *Plantago asiatica* in rats by liquid chromatography-mass spectrometry. *J Pharm Biomed Anal* 89: 251-256, 2014.
10. Demidenko ZN, Vivo C, Halicka HD, *et al*: Pharmacological induction of Hsp70 protects apoptosis-prone cells from doxorubicin: comparison with caspase-inhibitor- and cycle-arrest-mediated cytoprotection. *Cell Death Differ* 13: 1434-1441, 2006.
11. Chiu SJ, Lee MY, Chen HW, Chou WG and Lin LY: Germanium oxide inhibits the transition from G2 to M phase of CHO cells. *Chem Biol Interact* 141: 211-228, 2002.
12. Cathcart R, Schwiens E and Ames BN: Detection of picomole levels of hydroperoxides using a fluorescent dichlorofluorescein assay. *Anal Biochem* 134: 111-116, 1983.
13. Kurien BT and Scofield RH: Western blotting. *Methods* 38: 283-293, 2006.
14. Chinese Pharmacopoeial Commission: Pharmacopoeia of the People's Republic of China. Vol 1. People's Medical Publishing House, Beijing, China, p126, 2010.
15. Hu S, Sun W, Wei W, *et al*: Involvement of the prostaglandin E receptor EP2 in paeoniflorin-induced human hepatoma cell apoptosis. *Anticancer Drugs* 24: 140-149, 2013.
16. Tsuboi H, Hossain K, Akhand AA, *et al*: Paeoniflorin induces apoptosis of lymphocytes through a redox-linked mechanism. *J Cell Biochem* 93: 162-172, 2004.
17. Valko M, Rhodes CJ, Moncol J, Izakovic M and Mazur M: Free radicals, metals and antioxidants in oxidative stress-induced cancer. *Chem Biol Interact* 160: 1-40, 2006.
18. An Z, Qi Y, Huang D, *et al*: EGCG inhibits Cd(2+)-induced apoptosis through scavenging ROS rather than chelating Cd(2+) in HL-7702 cells. *Toxicol Mech Methods* 24: 259-267, 2014.
19. Yang HL, Chen CS, Chang WH, *et al*: Growth inhibition and induction of apoptosis in MCF-7 breast cancer cells by *Antrodia camphorata*. *Cancer Lett* 231: 215-227, 2006.
20. Kluck RM, Bossy-Wetzell E, Green DR and Newmeyer DD: The release of cytochrome c from mitochondria: a primary site for Bcl-2 regulation of apoptosis. *Science* 275: 1132-1136, 1997.
21. Ryan KM, Phillips AC and Vousden KH: Regulation and function of the p53 tumor suppressor protein. *Curr Opin Cell Biol* 13: 332-337, 2001.
22. Junttila MR, Li SP and Westermarck J: Phosphatase-mediated crosstalk between MAPK signaling pathways in the regulation of cell survival. *FASEB J* 22: 954-965, 2008.
23. Pu X, Song Z, Li Y, Tu P and Li H: Acteoside from *Cistanche salsa* inhibits apoptosis by 1-methyl-4-phenylpyridinium ion in cerebellar granule neurons. *Planta Med* 69: 65-66, 2003.